

**REGIONAL LOCATION CALIBRATION IN ASIA**

Lee Steck, Hans Hartse, Chris Bradley, Claudia Aprea, Aaron Velasco, George Randall, and Jill Franks

Los Alamos National Laboratory

Sponsored by National Nuclear Security Administration  
Office of Nonproliferation Research and Engineering  
Office of Defense Nuclear Nonproliferation

Contract No. W-7405-ENG-36

**ABSTRACT**

Seismic event location for global nuclear explosion monitoring is a multi-faceted problem. This paper presents a spectrum of issues and efforts involved in improving location performance worldwide. Our efforts are largely designed around providing validated, rigorously calibrated travel times, azimuths, and slownesses along with accurate error estimates. To do so entails a significant effort that includes data mining, data integration, database management, developing optimal 1-, 2-, and 3-D Earth models, using the Earth models to predict wave propagation, developing corrections and errors for travel times, azimuths, and slownesses, and validation of all products. Results presented here will focus on Asia.

Previous work has shown that non-stationary modified Bayesian kriging of travel-time residuals successfully improves regional seismic event location, and this method is being extended to calculate corrections for azimuth and slowness. The ability to krig over 3-D Earth models is also being implemented. In order to produce the most useful corrections, we require accurate ground truth. For this we are continuing efforts to create a location database consisting of the best available seismic event locations and the most accurate and precise travel times. Building this database relies on participation from universities, other National Nuclear Security Administration (NNSA) laboratories, and contacts in private industry. Through the kriging procedure we are able to stabilize location algorithms, but the ultimate usefulness of the corrections themselves is directly related to the quality of the ground truth from which the corrections are derived. Indeed, epicentral mislocations from location algorithms (EvLoc) using travel-time correction surfaces are directly proportional to the location errors of the ground truth used to generate the corrections.

In aseismic regions, corrections for travel time, azimuth, and slowness are predicted from optimal Earth models using one of the following methods, depending on application: TauP, ray bending, reflectivity, or finite difference. We have developed a model-building tool that can incorporate many different types of data, from surfaces (Moho, bathymetry, topography), to local or regional 1-, 2-, and 3-D models, to reflection profiles, to point data. Numbers of layers are defined within prominent sections of the lithosphere, and interpolation between data points is used to create a smooth, self-consistent 3-D Earth model.

## ***24th Seismic Research Review – Nuclear Explosion Monitoring: Innovation and Integration***

### **OBJECTIVE**

The objective of this work is to improve seismic event location in Asia. We achieve our objective through a multi-faceted approach encompassing database development, data integration, geophysical model building, numerical simulation of wave propagation, travel-time kriging, location algorithm development, and validation.

### **RESEARCH ACCOMPLISHED**

A new location database is being compiled to provide a preferred origin and a superset of arrivals compiled from all available global and regional catalogs. The effort has focused on merging global and regional seismic event bulletin information with Los Alamos National Laboratory (LANL)-generated phase arrival and waveform data using a combination of PERL scripts and the ORLoader codes. The result is a set of database tables that contain integrated seismic event data from many sources. These tables are the foundation for the creation of CSS3.0 *assoc* and *arrival* tables that will be used specifically for event relocations. Merging event bulletins and renaming of seismic phases follow separate pre-determined ranking schemes. As of this writing, we have about 600,000 preferred origins and 14,000,000 arrivals (excluding ISC and LANL picks). Of these arrivals, 8,500,000 are either P or Pn. About 150,000 waveforms have been tied to the database (748 from chemical explosions; 1086 from nuclear explosions) and 45,000 picks are being incorporated from LANL (see also Begnaud *et al*, this volume).

The InSAR component of our ground truth acquisition effort has produced some interesting global and regional results. Figure 1 shows theoretical predictions of ground displacement for several different fault orientations and depths. These results are used along with statistical seismicity patterns derived from the PDE catalog to predict the number of InSAR-observable earthquakes per year on a 2.5° grid around the globe (Figure 2) (Earle and Cogbill, submitted manuscript). These results seem encouraging on the whole, but in a follow-on study in China, a number of problems were encountered that illustrate the difficulties in applying InSAR to smaller events (see Peltzer *et al.*, 2001). A major difficulty with the area around China is the limited number of satellite download stations. Other problems arise from the high mountainous terrain and associated precipitation that can produce undesired signals. Figure 3 illustrates an InSAR result for a moderate-sized event in China.

We have completely revised and extended our regionalization of Asia to include southern Asia, northeast Russia, the Aleutian Islands, and Alaska (Figure 4). The principal changes in China were to combine some of the smaller and/or irregular provinces into more geophysically useful regions. The digitized provinces were defined based on the Exxon geologic maps. Our 3-D Asia model will be updated with these provinces using Litho3D and Model3D. Appropriate regional crustal models are inserted into the provinces and the 3SMAC model is used for the mantle.

Our modeling tool has been adapted to allow computation of 3-D travel times from any event to any station with no need to convert the output model to any other format. We have been using a 3-D bending method for computing minimum travel times, based on Steck and Prothero (1991). This code has been modified to perform in a 3-D spherical model, with topography. We have been exploring the validation of one of our *a-priori* models using this technique. The results allow us to explore which parts of any *a priori* model perform better (or worse) than IASPEI91 (or any other model). We have also included a new visualization tool: we can define a great circle transect from one station to any part of the model, and the code generates a 2-D cross-section. An additional, more qualitative assessment tool for validating models is developed using a wave front construction code (Hildebrand *et al*, 1999). This code has been also modified to perform in a 3-D spherical Earth. The wave front is constructed from interpolation of rays calculated via the shooting method.

As part of our regionalization effort, we have performed a literature search to gather velocity models from regional distances around MAKZ, a seismic array near Makanchi. As of this writing, we have compiled roughly 30 velocity models for the Tien Shan, Kazakhstan, and Siberian shield regions. These are being tested against data to determine the best fitting 1-D models. Eight Vp/Vs models have been gathered for eastern Kazakhstan, and these are shown in Figure 5.

To aid in our Asia calibration efforts, we are analyzing Makanchi and Karatau array data for FK performance and azimuth corrections. With only a handful of events analyzed, no major azimuthal perturbations are observed. Figure 6 shows an example of azimuth and slowness determined for an event recorded at MKAR. We have coded up the

## ***24th Seismic Research Review – Nuclear Explosion Monitoring: Innovation and Integration***

pseudo-FK method, and have implemented improvements in both the error calculation as well as the peak energy calculation.

While correction surfaces are being compiled for stations of interest in Asia using NMBK (Schultz *et al*, 1999), we are also looking towards implementing new methods for locating events. Figure 7 shows a comparison between double-difference relocations and EvLoc relocations for an earthquake sequence in Tibet. Methods of optimizing the double difference and related correlation methods for seismic event relocation are being sought.

### **CONCLUSIONS AND RECOMMENDATIONS**

We are making headway in solving the location problem in Asia. The task is a vast one, and a successful program requires the mutual cooperation of the Department of Energy/NNSA and Department of Defense efforts and the Air Force Technical Applications Center, along with universities and private companies. Results presented in this paper are a snapshot of recent progress in some of our research areas and further work will be presented at the 24<sup>th</sup> Seismic Research Review.

### **REFERENCES**

- Belyashova, N.N., V.I. Shacilov, N.N. Mikhailova, I.I. Komarov, Z.I. Sinyova, A.V. Belyashov, and M.N. Malakhova, On the Use of Calibration Explosions at the Former Semipalatinsk Test Site for Compiling a Travel-time Model of the Crust and Upper Mantle, *Pure Appl. Geophys.*, **158**, 193-209, 2001.
- Egorkin, A.V., Velocity structure, composition and discrimination of crustal provinces in the former Soviet Union, *Tectonophysics*, **298**, 395-404, 1998.
- Ghose, S., M.W. Hamburger, and J. Virieux, Three-dimensional velocity structure and earthquake Locations beneath the northern Tien Shan of Kyrgyzstan, central Asia, *J. Geophys. Res.*, **103**, 2725-2748, 1998.
- Hildebrand S, M. Fehler, and C. Aprea (1999), Wavefront Construction: A Differential Geometry Approach, *SGL*, **70**, 199-206.
- Jih, R.S., Location Calibration efforts in China, in Proceedings of the 20th Annual Seismic Research Symposium in Monitoring a Comprehensive Test Ban Treaty, 21-23 Sept 1998.
- Kosarev, G.L., N.V. Petersen, L.P. Vinnik, and S.W. Roecker, Receiver functions for the Tien Shan analog broadband network: contrasts in the evolution of structures across the Talasso-Fergana Fault, *J. Geophys. Res.*, **98**, 4437-4448, 1993.
- Mangino, S., K. Priestley, and J. Ebel, The receiver structure beneath the China Digital Seismograph Network Stations, *Bull. Seismol. Soc. Am.*, **89**, 1053-1076, 1999.
- Morozova, E.A., I.B. Morozov, S.B. Smithson, and L.N. Solodilov, Heterogeneity of the uppermost mantle beneath Russian Eurasia from the ultra-long-range profile QUARTZ, *J. Geophys. Res.*, **104**, 20329-20348, 1999.
- Petit, C., and J. Deverchere, Velocity structure of the northern Baikal rift, Siberia, from local and regional earthquake travel times, *Geophys. Res. Lett.*, **22**, 1677-1680, 1995.
- Priestley, K.F., G. Zandt, and G.E. Randall, Crustal structure in eastern Kazakh, USSR from teleseismic receiver functions, *Geophys. Res. Lett.*, **15**, 613-616, 1988.
- Priestley, K., J. Cipar, A. Egorkin, and N. Pavlenkova, Upper-mantle velocity structure beneath the Siberian platform, *Geophys. J. Int.*, **118**, 369-378, 1994.

Roecker, S.W., T.M. Sabitova, L.P. Vinnik, Y.A. Burmakov, M.I. Golvanov, R. Mamatkanova, and L. Munirova, Three-Dimensional Elastic Wave Velocity Structure of the Western and Central Tien Shan, *J. Geophys. Res.*, **98**, 15779-15795, 1993.

Schultz, C., S. Myers, J. Hipp, and C. Young (1998), Nonstationary Bayesian Kriging: Application of Spatial Corrections to Improve Seismic Detection, Location and Identification, *Bull. Seism. Soc. Am.*, 1275-1288.

Steck, L. and W. A. Prothero, 1991. A 3-D raytracer for teleseismic body-wave arrival times, *Bull. Seis. Soc. Am.*, **81**, 1332-1339.

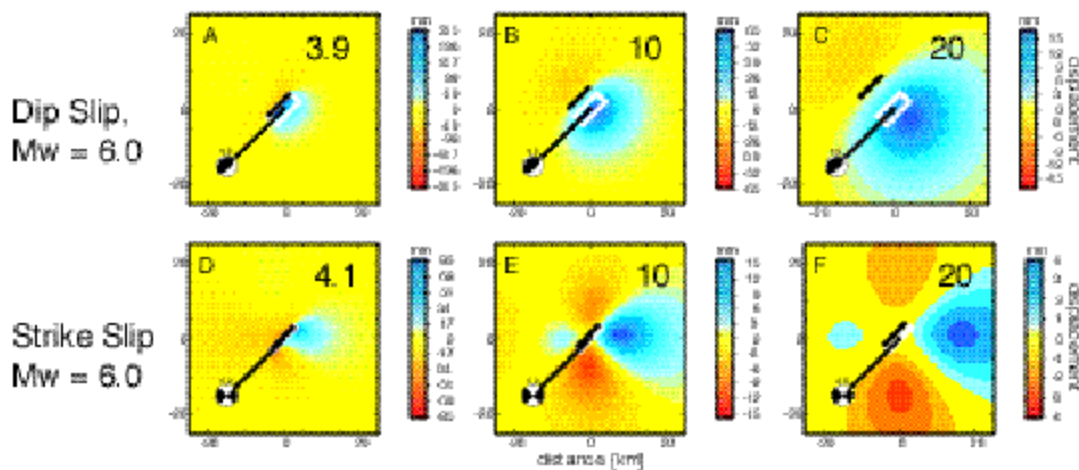
Thurber, C., H. Given, and J. Berger, Regional seismic event location with a sparse network: application to eastern Kazakhstan, USSR, *J. Geophys Res.*, **94**, 17767-17780, 1989.

Thurber, C., C. Trabant, F. Haslinger, and R. Hartog, Nuclear explosion locations at the Balapan, Kazakhstan, nuclear test site: the effects of high-precision arrival times and three-dimensional structure, *phys. Earth Planet. Inter.*, **123**, 283-301, 2001.

Whitted, C.A., S.R. Taylor, A.A. Velasco, H.E. Hartse, and G. Zandt, A path specific study in central Asia from group velocity inversions and full waveform modeling, Los Alamos National Laboratory, LAUR-99-3040, 19 pp.

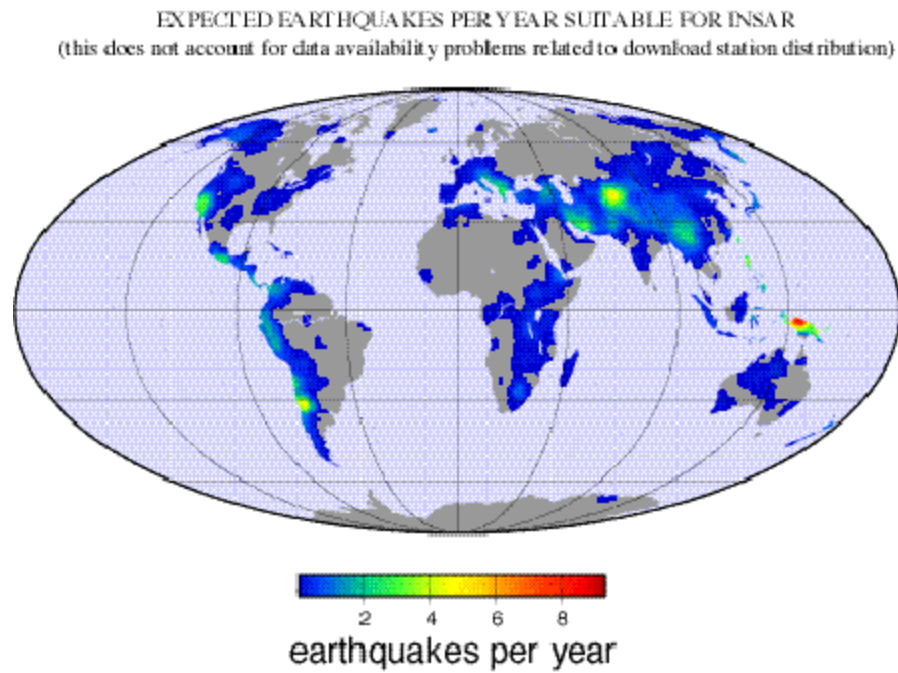
### THEORETICAL ELASTIC DISPLACEMENT AMPLITUDES

Calculated from elastic dislocation theory (Okada, 1985).  
 Need 3 cm displacement to observe with InSAR.  
 C, E, F are not detectable.



(From Earle and Cogbill, BSSA, submitted manuscript)

**Figure 1.** Plot showing theoretical line-of-sight co-seismic surface displacement in millimeters for dip-slip and strike-slip events. The white lines show the surface projection of the square fault planes, and the black lines show the surface trace of the fault. All displacements were calculated for  $M = 6.0$ . The centroid depths are A) 3.9 km, B) 10 km, C) 20 km, D) 4.3 km, E) 10 km, and F) 20 km. The dip-slip events (A, B, and C) all have a dip of  $67^\circ$  and the strike-slip events (D, E, and F) have a dip of  $85^\circ$ . The events C, E, and F lie outside the detection threshold.



(From a manuscript by Paul Earle (USGS) and Allen Cogbill (LANL), 2002.)

**Figure 2.** The number of magnitude 5.0 and greater shallow earthquakes occurring per year in a circle of radius  $2.5^\circ$ . The map was generated by calculating earthquake frequency within overlapping  $2.5^\circ$  radius caps and then smoothing the result. The frequency was obtained from 27 years of PDE data.

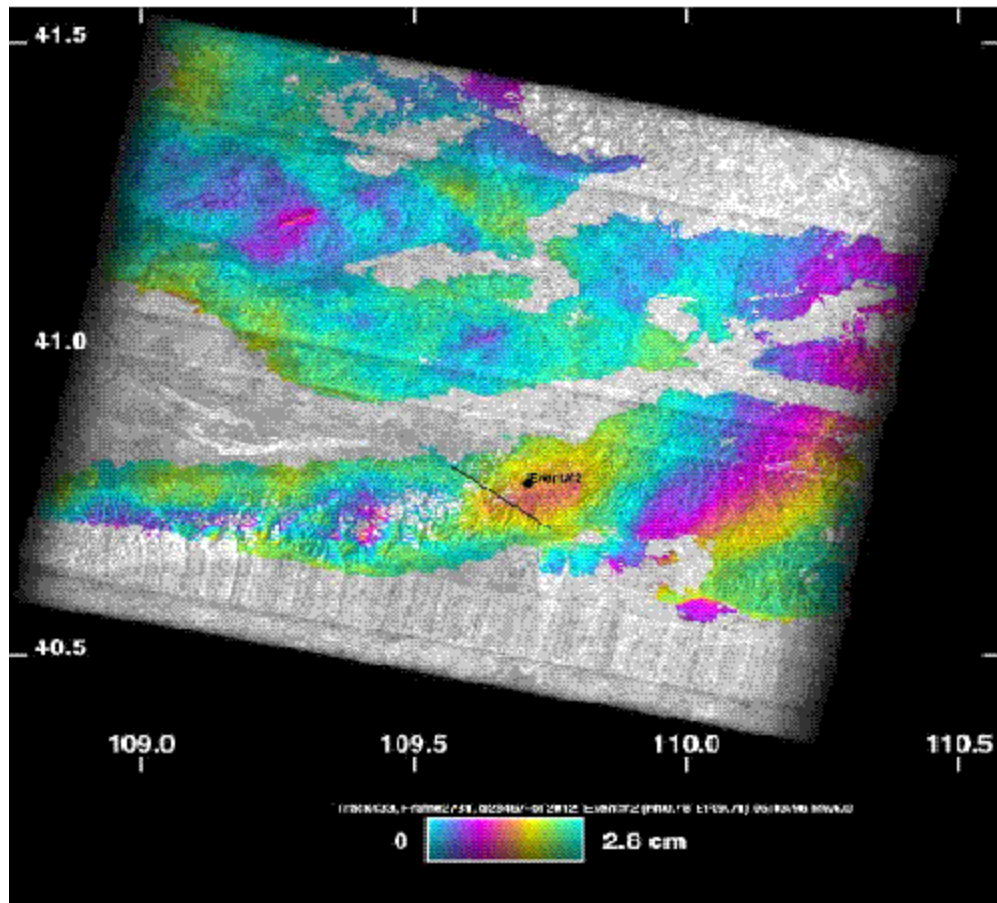


**Figure 3.** InSAR results for a moderate sized event in China, Mw 6.0. This was deemed a successful result, the only success in attempting to look at three Mw 5-6 events in China.

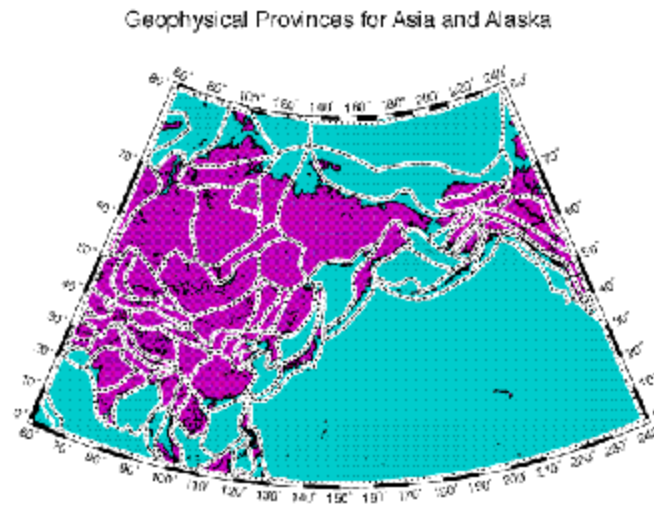


Figure 4. Our newly updated geophysical provinces for Asia and environs.

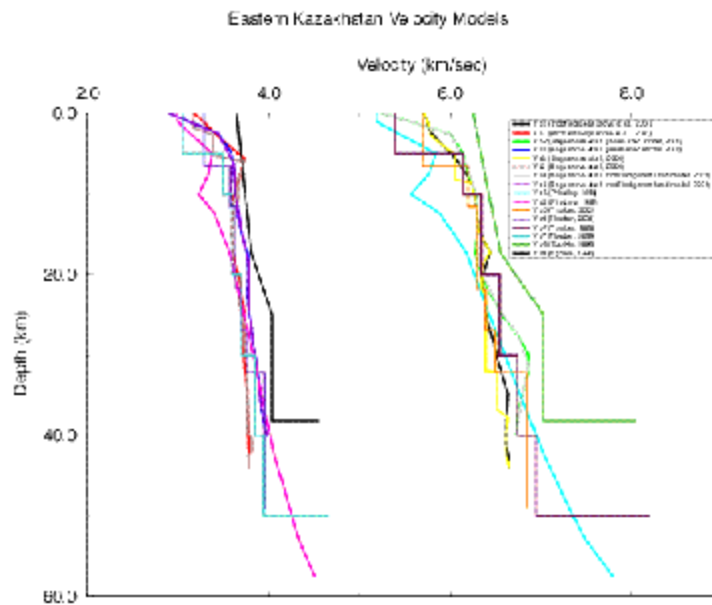


Figure 5. Sample velocity models for eastern Kazakhstan.

Event: 9/12/2000, 0:28:02.03, M5.7  
 lat 35.373, lon 99.343, BAZ=125.6

MKAR FK RESULT:

Maximum Value: Slowness = 0.12207, Azimuth = 124.992

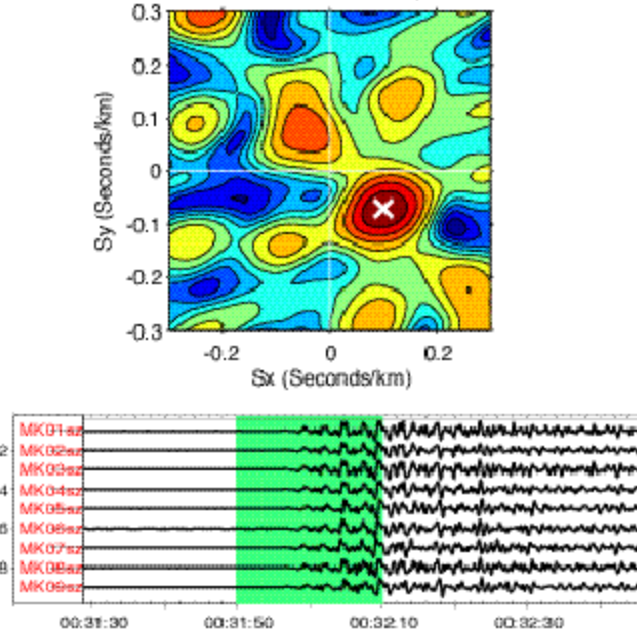


Figure 6. Pseudo FK result for station MKAR.

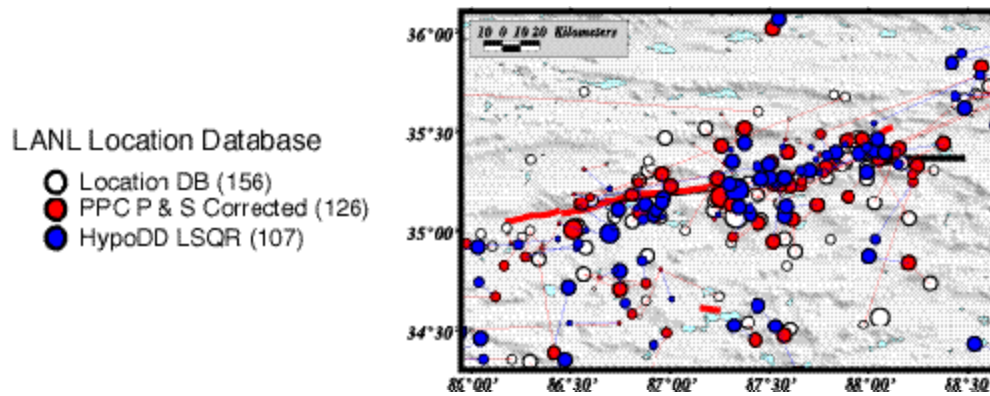


Figure 7. Comparison of EvLoc, EvLoc plus P and S corrections, and Double Difference locations.